P3H–23–046, TTP23–026

Electric Dipole Moments as Probes of B Anomaly

Syuhei Iguro[1, 2, *] and Teppei Kitahara[3, 4, †]

[1] *Institute for Theoretical Particle Physics (TTP), Karlsruhe Institute of Technology (KIT),*
Wolfgang-Gaede-Str. 1, 76131 Karlsruhe, Germany
[2] *Institute for Astroparticle Physics (IAP), Karlsruhe Institute of Technology (KIT),*
Hermann-von-Helmholtz-Platz 1, 76344 Eggenstein-Leopoldshafen, Germany
[3] *CAS Key Laboratory of Theoretical Physics, Institute of Theoretical Physics,*
Chinese Academy of Sciences, Beijing 100190, China
[4] *Kobayashi-Maskawa Institute for the Origin of Particles and the Universe, Nagoya University, Nagoya 464–8602, Japan*

The measurements of the lepton flavor universality (LFU) in $\mathcal{B}(\overline{B} \to D^{(*)} l \overline{\nu})$ indicate a significant deviation from the standard model prediction at a 3–4 σ level, revealing a violation of the LFU ($R_{D^{(*)}}$ anomaly). It is known that the $R_{D^{(*)}}$ anomaly can be easily accommodated by an $SU(2)_L$-singlet vector leptoquark (LQ) coupled primarily to third-generation fermions, whose existence is further motivated by a partial gauge unification. In general, such a LQ naturally leads to additional CP-violating phases in the LQ interactions. In this Letter, we point out that the current $R_{D^{(*)}}$ anomaly prefers the CP-violating interaction although $\mathcal{B}(\overline{B} \to D^{(*)} l \overline{\nu})$ is a CP-conserving observable. The CP-violating LQ predicts a substantial size of the bottom-quark electric dipole moment (EDM), the chromo-EDM, and also the tau-lepton EDM. Eventually, at low energy, the nucleon and electron EDMs are induced. Therefore, we conclude that the $R_{D^{(*)}}$ anomaly with the $SU(2)_L$-singlet vector LQ provides unique predictions: neutron and proton EDMs with opposite signs and a magnitude of $\mathcal{O}(10^{-27})\, e\,\mathrm{cm}$, with a null electron EDM signal. These EDMs could serve as crucial indicators in future experiments.

I. INTRODUCTION

In the near future, the sensitivities of precision measurements for the elementary particles, particularly B physics and the electric dipole moments (EDMs), are expected to be improved by an order of magnitude. Many kinds of new physics models will undoubtedly be probed through these improvements.

Currently, a significant deviation from the standard model (SM) prediction has been reported by the BaBar, LHCb, Belle, and Belle II experiments [1–13], in measurements of the lepton flavor universality (LFU) in $\overline{B} \to D^{(*)} l \overline{\nu}$. Violation of the LFU is represented by

$$R_{D^{(*)}} \equiv \frac{\mathcal{B}(\overline{B} \to D^{(*)} \tau \overline{\nu}_\tau)}{\mathcal{B}(\overline{B} \to D^{(*)} \ell \overline{\nu}_\ell)} \,, \tag{1}$$

where ℓ represents an average of the leptons. The up-to-date world average of the data [14, 15] is

$$R_D^{\mathrm{exp}} = 0.357 \pm 0.029 \,, \quad R_{D^*}^{\mathrm{exp}} = 0.284 \pm 0.012 \,, \tag{2}$$

while an up-to-date SM prediction [16–19] is

$$R_D^{\mathrm{SM}} = 0.290 \pm 0.003 \,, \quad R_{D^*}^{\mathrm{SM}} = 0.248 \pm 0.001 \,, \tag{3}$$

which implies more than 4σ level tension.

This $R_{D^{(*)}}$ anomaly naively suggests the existence of $\mathcal{O}(1)$ TeV new physics in the $b \to c \tau \overline{\nu}_\tau$ process, and various kinds of models have been proposed [19, 20]. A new physics candidate is an $SU(2)_L$-singlet vector leptoquark (LQ), dubbed as U_1 LQ. The U_1 LQ hypothesis has been widely discussed in connection with a partial gauge unification [21–23] as well as the related flavor processes and the LHC phenomenology have been studied [24, 25]. These new physics predictions will be tested in the ongoing Belle II [26] and LHCb experiments [27]. One should note that to avoid the strict constraint from $K_L \to \mu e$ measurements [28, 29], (elaborate) $U(2)$ flavor symmetries have been considered for a successful interpretation of the $R_{D^{(*)}}$ anomaly [30–33]. In that case, the U_1 LQ couples primarily to third-generation fermions.

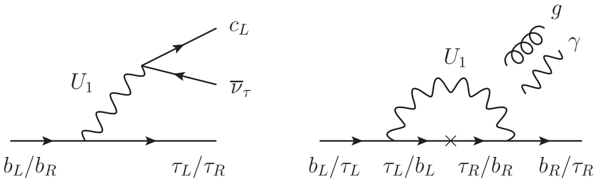

FIG. 1. The vector-LQ (U_1) contributions to $R_{D^{(*)}}$ (left diagram) and the (chromo-) EDMs for the bottom-quark and tau-lepton (right diagram).

The LQ model naturally brings a CP-violating (CPV) phase, which comes from the rotation matrices to the mass bases of the left- and right-handed quark and lepton fields that are not aligned in general. In this Letter, it will be clarified that the CPV phase is necessary to accommodate the $R_{D^{(*)}}$ anomaly, and this phase also induces the sizable nucleon EDMs at the low energy, which will be testable in the near future (see Fig. 1 for the Feynman diagrams). Although Refs. [34, 35] investigated the EDMs in the vector-LQ model in light of the $R_{D^{(*)}}$ anomaly, they focused on the parameter benchmark points and the necessity of the CPV phase was unclear. On the other hand, it is known that there is no robust correlation be-

---

[*] igurosyuhei@gmail.com
[†] teppeik@itp.ac.cn

tween the $R_{D^{(*)}}$ anomaly and EDMs in scalar LQ models [34, 36–39].

II. LQ MODEL

We consider a simplified U_1 LQ scenario with a $U(2)$ flavor symmetry. The relevant fermion interactions are described by

$$\mathcal{L} = \left(\beta_L^{ij}\overline{Q}_i\gamma_\mu P_L L_j + \beta_R^{ij}\overline{d}_i\gamma_\mu P_R e_j\right) U_1^\mu + \text{h.c.}\,, \tag{4}$$

with $P_{L/R} = (1 \mp \gamma_5)/2$ in the fermion mass eigenbasis. Although additional vector-like fermions are needed in Eq. (4) to obtain the ideal flavor structure in the UV complete model [40], we focus on the 3×3 flavor structures. This simplification is valid to consider the EDMs, and we will discuss this point in Sec. III D.

We consider the following flavor texture [23, 40]

$$\begin{aligned} \beta_L^{ij} &\simeq \beta_L^{33}\begin{pmatrix} 0 & 0 & -c_d s_{q_2} s_\chi \left|\frac{V_{td}}{V_{ts}}\right| \\ 0 & 0 & c_d s_{q_2} s_\chi \\ 0 & 0 & c_\chi \end{pmatrix}\,, \\ \beta_R^{ij} &\simeq \beta_L^{33} e^{i\phi_R}\begin{pmatrix} 0 & 0 & 0 \\ 0 & 0 & 0 \\ 0 & 0 & 1 \end{pmatrix}\,, \end{aligned} \tag{5}$$

where $c_d \simeq 0.98$, corresponding to a case of $s_{l_2} \simeq s_\tau \simeq 0$ in the literature. Here, s_i and c_i represent flavor rotations $\sin\theta_i$ and $\cos\theta_i$ to bring the SM fermions to their mass eigenbasis. Note that $|\beta_L^{33}| \simeq |\beta_R^{33}|$ results from the gauge symmetry in the UV complete model. In this setup, ϕ_d is an arbitrary CPV phase; the other CPV phases can be absorbed by a redefinition of ϕ_d [41]. Therefore, the relative phase between β_L and β_R interactions plays an important role in the CPV observables.

In our analysis, only three parameters are relevant to the phenomenology: β_L^{33}/m_{U_1}, $\beta_L^{23}/\beta_L^{33}(= c_d s_{q_2} s_\chi/c_\chi)$, and ϕ_R.

III. EDMS AND OTHER OBSERVABLES

In this section, we concisely summarize the phenomenological effects of the U_1 LQ.

First, we focus on the LQ contributions to EDMs. The effective Lagrangian for the EDM (d_f) and chromo-EDM interactions ($\tilde{d}_f$) are expressed as

$$\mathcal{L}_{\text{eff}} = -\frac{i}{2}\sum_f\left(d_f\overline{f}\sigma_{\mu\nu}\gamma_5 f F^{\mu\nu} + g_s\tilde{d}_f\overline{f}\sigma_{\mu\nu}T^a\gamma_5 f G^a_{\mu\nu}\right)\,, \tag{6}$$

with $\sigma_{\mu\nu} = \frac{i}{2}[\gamma_\mu, \gamma_\nu]$. Based on Refs. [35, 42, 43], the U_1 LQ contributions to the tau-lepton and bottom-quark (chromo-) EDMs are (see Fig. 1 right diagram)

$$d_\tau = -\frac{3e}{8\pi^2}\frac{m_b}{m_{U_1}^2}\text{Im}\left[\beta_L^{33}(\beta_R^{33})^*\right]\,, \tag{7}$$

$$d_b(\Lambda_{\text{LQ}}) = -\frac{5e}{24\pi^2}\frac{m_\tau}{m_{U_1}^2}\text{Im}\left[\beta_L^{33}(\beta_R^{33})^*\right]\,, \tag{8}$$

$$\tilde{d}_b(\Lambda_{\text{LQ}}) = -\frac{1}{8\pi^2}\frac{m_\tau}{m_{U_1}^2}\text{Im}\left[\beta_L^{33}(\beta_R^{33})^*\right]\,, \tag{9}$$

and there is no contribution to the other EDMs at the LQ mass scale, $\mu = \Lambda_{\text{LQ}}$. Note that the Weinberg operator ($GG\tilde{G}$) would be induced at two-loop level, but it is suppressed by $m_b m_\tau/m_{U_1}^4$, and we discarded it [37]. While there is no QCD renormalization-group (RG) evolution for d_τ, we have taken into account the RG evolutions from Λ_{LQ} to $\mu_b(= m_b)$ [38, 44], which are known to relax the EDM bound [45]. For example, the RG evolutions provide the following corrections:

$$d_b(\mu_b) = 0.84\, d_b(\Lambda_{\text{LQ}}) - 0.42e\,\tilde{d}_b(\Lambda_{\text{LQ}})\,, \tag{10}$$

$$\tilde{d}_b(\mu_b) = 0.91\,\tilde{d}_b(\Lambda_{\text{LQ}})\,, \tag{11}$$

with $\Lambda_{\text{LQ}} = 2\,\text{TeV}$.

After integrating out the tau and bottom quark at low energy, the electron EDM is induced by the tau and bottom-quark EDMs from QED three-loop radiative corrections [46]. Furthermore, a semi-leptonic CP-odd operator, $(\overline{e}i\gamma_5 e)(\overline{p}p+\overline{n}n)$, is also induced by them from QED two-loop diagrams [47, 48], which eventually mimics the electron EDM (called an equivalent electron EDM) in the experiments [49, 50]. By using a result of the improved analysis for the QED three-loop calculation [51], we obtain

$$\begin{aligned} d_e = &\left[4.7 \times 10^{-13} + 8.8\,(1 \pm 0.1) \times 10^{-12}\right]\, d_b(\mu_b) \\ &+ \left(9.9 \times 10^{-12} + 9.2 \times 10^{-14}\right)\, d_\tau\,. \end{aligned} \tag{12}$$

Here, the first terms in each parenthesis come from the QED three-loop contribution, while the second terms come from the semi-leptonic CP-odd operator [48]. Note that the latter calculation is a result in the case of the HfF$^+$ molecule system [52] (see Refs. [49, 50] for the other molecules). The dominant theoretical uncertainty comes from the semi-leptonic CP-odd operator induced by the bottom-quark EDM, which is estimated as 10% [48].

By a similar but more involved process, the nucleon (neutron and proton) EDMs are induced from the bottom-quark EDM and chromo-EDM. Short-distance contributions come from the light-quark EDM and chromo-EDMs, d_N^{light}, and the Weinberg operator, d_N^{W} [53–55], while a long-distance contribution arises from a CP-odd photon-gluon operator ($GGG\tilde{F}$), $d_N^{\tilde{F}G^3}$ [48]. For

EDM [e cm]	90% CL limit	Future sensitivity
$\lvert d_e\rvert$	$\leq 4.1\times 10^{-30}$ [52]	$\mathcal{O}(10^{-31})$ [71]
$\lvert d_n\rvert$	$\leq 1.8\times 10^{-26}$ [72]	$\mathcal{O}(10^{-27})$ [73–76]
		$\mathcal{O}(10^{-28})$ [77]
$\lvert d_p\rvert$	$\leq 2.1\times 10^{-25}$ [78]	$\mathcal{O}(10^{-29})$ [79, 80]

TABLE I. The current 90% confidence level (CL) upper limits and future prospects for electron, neutron, and proton EDMs.

the neutron and proton EDMs, numerically we have

$$d_N = d_N^{\rm light} + d_N^{\rm W} + d_N^{\tilde{F}G^3} \qquad (\text{for } N=n,\,p)\,, \tag{13}$$

$$d_n^{\rm light} = 4.3\times 10^{-7} e\,\tilde{d}_b(\mu_b) + 4.2\times 10^{-8}\, d_b(\mu_b)\,, \tag{14}$$

$$d_p^{\rm light} = -3.6\times 10^{-7} e\,\tilde{d}_b(\mu_b) + 9.5\times 10^{-9}\, d_b(\mu_b)\,, \tag{15}$$

$$d_n^{\rm W} = -5.9\,(1\pm 0.5)\times 10^{-5} e\,\tilde{d}_b(\mu_b)\,, \tag{16}$$

$$d_p^{\rm W} = 8.5\,(1\pm 0.5)\times 10^{-5} e\,\tilde{d}_b(\mu_b)\,, \tag{17}$$

$$d_N^{\tilde{F}G^3} \approx 7\times 10^{-7}\, d_b(\mu_b) \qquad (\text{for } N=n,\,p)\,. \tag{18}$$

For $d_N^{\rm light}$, the QCD sum-rule estimate is used [50, 56–59] (where the Peccei-Quinn mechanism is assumed to suppress a $\bar{\theta}$ term), whose overall normalization is determined by the lattice result [60]. The light-quark EDMs are induced by the bottom-quark EDM [48] and chromo-EDM [51], while the light-quark chromo-EDMs are induced from the bottom-quark chromo-EDM [44]. For $d_N^{\rm W}$, the QCD sum-rule estimates [50, 61, 62] (see also [63]) are used. Note that although all the above terms have 10%–30% theoretical uncertainties, we suppressed them except for the leading one. For $d_N^{\tilde{F}G^3}$, the QCD sum-rule technique is also used and the numerics should be understood as an order-of-magnitude estimation [48].

It is found that the overwhelmingly dominant contribution to the nucleon EDMs comes from the Weinberg operator. Also, the theoretical uncertainty is dominated by the Weinberg operator, which is estimated as 50% [62]. Although the accuracy of the lattice calculations is currently not competitive [64–70], they will provide complementary inputs in the future. We emphasize that the predicted neutron and proton EDMs must be the same size with opposite signs [62].

The current bounds and the future prospects for the electron, neutron, and proton EDMs are summarized in Table I.

A. $R_{D^{(*)}}$

The U_1 LQ can naturally explain the $R_{D^{(*)}}$ anomalies. After integrating out the LQ and the weak bosons, the effective Lagrangian is given by

$$\mathcal{L}_{\rm eff} = -2\sqrt{2}G_F V_{cb}\left[(1+C_{V_L})\,O_{V_L} + C_{S_R}O_{S_R}\right]\,, \tag{19}$$

with

$$O_{V_L} = (\bar{c}\gamma^\mu P_L b)(\bar{\tau}\gamma_\mu P_L \nu_\tau)\,,\ \ O_{S_R} = (\bar{c}P_R b)(\bar{\tau}P_L\nu_\tau)\,. \tag{20}$$

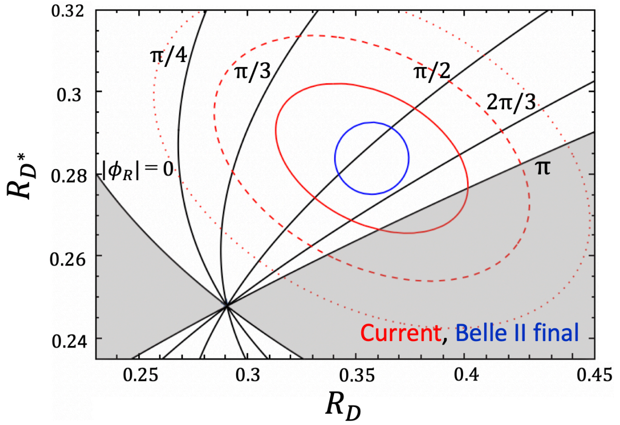

FIG. 2. The black contour represents the CPV phase $|\phi_R|$ on the plane of R_D–R_{D^*}. The red solid, dashed, and dotted contours correspond to 1, 2, 3σ of the experimental world average [15]. The blue circle denotes a sensitivity projection of the Belle II experiment [26] assuming the current central values. The gray-shaded region is out of the model prediction.

and the Wilson coefficients (WCs) at $\mu=\mu_b$ are

$$C_{V_L}(\mu_b) = \frac{\eta_{V_L}}{2\sqrt{2}G_F V_{cb}}\frac{\beta_L^{23}(\beta_L^{33})^*}{m_{U_1}^2}\,, \tag{21}$$

$$C_{S_R}(\mu_b) = -\frac{\eta_{S_R}}{\sqrt{2}G_F V_{cb}}\frac{\beta_L^{23}(\beta_R^{33})^*}{m_{U_1}^2}\,, \tag{22}$$

where η_{V_L} and η_{S_R} are coefficients of the QCD corrections [81–83]. For $\Lambda_{\rm LQ}\simeq$ 2–4 TeV, $\eta_{V_L}\simeq 1.1$ and $\eta_{S_R}\simeq 2.0$ [19]. Furthermore, assuming the simplified flavor texture in Eq. (5), these two WCs can be correlated with being

$$C_{S_R}(\mu_b) \simeq -3.6\,e^{-i\phi_R}C_{V_L}(\mu_b)\,. \tag{23}$$

By using the numerical formulae for $R_{D^{(*)}}$ in Ref. [19], based on the heavy quark effective theory form factors [17], we show a correlation between $R_{D^{(*)}}$ and the CPV phase ϕ_R in Fig. 2. Since $R_{D^{(*)}}$ are the CP-conserving observables, they depend on only $\cos\phi_R$ and are invariant under $\phi_R \leftrightarrow -\phi_R$. The black contour denotes the values of $|\phi_R|$ with varying β_L^{33}/m_{U_1}. We use $\beta_L^{23}/\beta_L^{33} = \lambda \simeq 0.225$ as a typical reference value [40]. The gray-shaded region cannot be predicted within the U_1 LQ model. It is found that large ϕ_R ($\pi/3 < |\phi_R|$) is favored to accommodate the $R_{D^{(*)}}$ anomaly, while a CP-conserving scenario of $\phi_R = 0$ can be excluded by the current data. One should note that the U_1 LQ model also leads to deviations from the SM predictions in other $b\to c\tau\bar{\nu}$ observables, τ polarization asymmetry and the LFU violation in $\Lambda_b \to \Lambda_c l\bar{\nu}$, which will be shown in Appendix A.

B. $B_s \to \tau^+\tau^-$

Within the SM, $B_s\to\tau^+\tau^-$ is suppressed by the one-loop factor and also the chirality factor, $m_\tau^2/m_{B_s}^2$. On the other hand, the U_1 LQ contributions are induced at

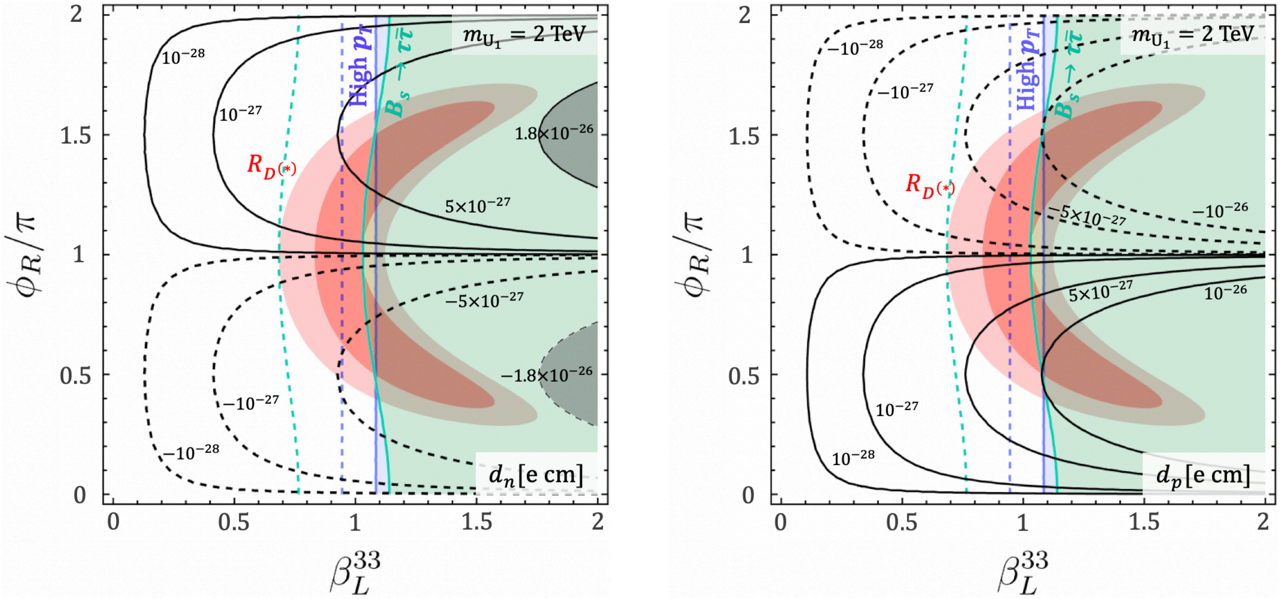

FIG. 3. The predicted neutron and proton EDMs are shown by the black contours in the left and right panels, respectively, where the solid (dashed) lines represent positive (negative) EDMs. The red (light red) region can explain the $R_{D^{(*)}}$ anomaly at 1σ (2σ) level. The blue and green regions are excluded by the high-p_T bound and $B_s \to \tau^+\tau^-$, respectively. The estimated sensitivities based on upcoming Run 3 data are shown by the dashed blue and green lines. We set $m_{U_1} = 2\,\mathrm{TeV}$ and $\beta_L^{23}/\beta_L^{33} = \lambda$.

the tree level and further the chirality suppression can be avoided. Therefore, $B_s \to \tau^+\tau^-$ is significantly affected by the LQ. Currently, the LHCb with Run 1 data sets the upper limit on the branching ratio at 95 % CL as [84]

$$\mathcal{B}(B_s \to \tau^+\tau^-) \leq 6.8 \times 10^{-3}\,. \tag{24}$$

The future prospect of the LHCb Run 3 has been estimated to improve the sensitivity by a factor of five [85]. The U_1 LQ contribution to $B_s \to \tau^+\tau^-$ including the QCD corrections is give by [40]

$$\begin{aligned}&\frac{\mathcal{B}(B_s \to \tau^+\tau^-)}{\mathcal{B}(B_s \to \tau^+\tau^-)^{\rm SM}}\\ &\simeq \left|1 + \frac{\pi}{\sqrt{2}\alpha G_F V_{tb}V_{ts}^* m_{U_1}^2}\beta_L^{23}\left(-0.26\beta_L^{33} + 1.8\beta_R^{33}\right)^*\right|^2\\ &\quad + \left(1 - \frac{4m_\tau^2}{m_{B_s}^2}\right)\left|\frac{1.8\pi}{\sqrt{2}\alpha G_F V_{tb}V_{ts}^* m_{U_1}^2}\beta_L^{23}(\beta_R^{33})^*\right|^2\,. \end{aligned}\tag{25}$$

It is noted that the effect from the CPV phase ϕ_R is mild due to the smallness of the SM contribution.

C. LHC high-p_T bound

We employed a public tool `HighPT` [86] to derive the collider constraint from $pp \to \tau^+\tau^-$ and $pp \to \tau\nu$ data. Currently, the dominant constraint comes from the high-p_T di-τ search from the ATLAS collaboration [87] (see also Refs. [88, 89] for the relevant study). At the CMS, an excess has been found in the high-p_T tail region [90, 91]. However, the ATLAS does not find excess in the region.[#1] On the other hand, the constraint from high-p_T mono-τ search is currently less constraining [93, 94]. However, it has been pointed out that requiring an additional b-tagged jet can improve the sensitivity so that this channel is competitive with the di-τ channel [95, 96].

D. Comment on other constraints

It is known that although loop-induced LQ contributions to $B_s - \overline{B}_s$ mixing mixing give a severe constraint, once additional vector-like fermions are introduced in the UV complete model the constraint can be naturally avoided thanks to the GIM-like mechanism [24, 40, 97–101]. We emphasize that the vector-like fermions do not mix the SM right-handed fermions in the UV complete model, and the EDMs are not induced from the vector-like fermion loops [40]. Therefore, the EDMs provide a unique prediction of the model.

The similar sensitivity to $B_s \to \tau^+\tau^-$ could be obtained from the measurement of $B \to K\tau^+\tau^-$ at the Belle II [25], while we omitted it since the current bound is much weaker. Although $B^- \to \tau\overline{\nu}$ is also modified in the simplified flavor texture, a moderate β_L^{13} suppresses the constraint [40].

[#1] More detailed experimental comparisons and/or statistics are necessary to conclude the difference between the CMS and ATLAS results [92].

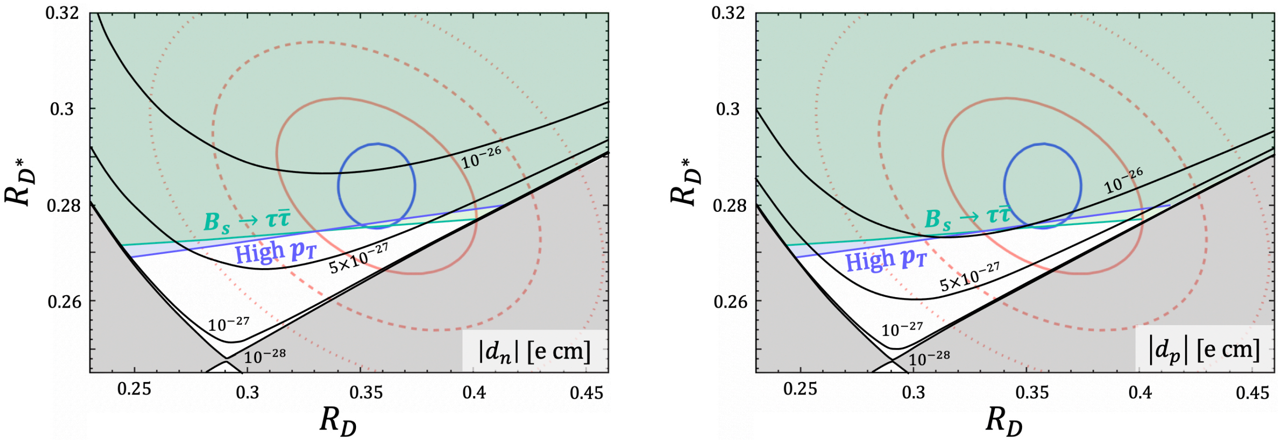

FIG. 4. The absolute values of the predicted neutron and proton EDMs are shown by the black contours in the left and right panels, respectively. Constraints from the high-p_T search and $B_s \to \tau^+\tau^-$ are represented by the blue and green regions, respectively. The gray-shaded regions are out of the model prediction. We set $m_{U_1} = 2\,\mathrm{TeV}$ and $\beta_L^{23}/\beta_L^{33} = \lambda$.

IV. RESULT

In Figs. 3 and 4, we show the correlations between the predicted nucleon (neutron and proton) EDMs and the $R_{D^{(*)}}$ anomaly in the U_1 LQ model. Here, $m_{U_1} = 2\,\mathrm{TeV}$ and $\beta_L^{23}/\beta_L^{33} = \lambda$ are taken as reference values. Black contours in Fig. 3 indicate the neutron and proton EDMs in the left and right panels, respectively, where the solid (dashed) lines represent positive (negative) EDMs. We used the central values of Eqs. (16) and (17) for the estimates of the nucleon EDMs. The blue and green regions are excluded by the high-p_T bound and $B_s \to \tau^+\tau^-$, respectively. The estimated sensitivities based on upcoming Run 3 data are shown by the dashed blue and green lines in Fig. 3. We also show the correlations on the R_D–R_{D^*} plane in Fig. 4.

These figures show that some of the preferred areas are already excluded by both the high-p_T bound and $B_s \to \tau^+\tau^-$. In the allowed regions, the predicted magnitudes of the nucleon EDMs are $|d_n| < 7 \times 10^{-27}\,e\,\mathrm{cm}$ and $|d_p| < 1 \times 10^{-26}\,e\,\mathrm{cm}$. Very excitingly, in the near future, several experiments will probe the neutron EDM at $\mathcal{O}(10^{-27})\,e\,\mathrm{cm}$ precision [73–76], and eventually $\mathcal{O}(10^{-28})\,e\,\mathrm{cm}$ [77]. Furthermore, two experiments are proposed that the proton EDM will be proved at $\mathcal{O}(10^{-29})\,e\,\mathrm{cm}$ precision [79, 80]. Therefore, we conclude that neutron and proton EDMs and their opposite signs will be a smoking-gun signal of the U_1 LQ model.

On the other hand, the induced electron EDM from Eq. (12) is $|d_e| < 10^{-32}\,e\,\mathrm{cm}$, which is a few orders away from the future prospect, but the suppressed electron EDM is also a unique prediction of this model.

V. SUMMARY AND DISCUSSION

In this Letter, we established a robust bridge between the electric dipole moments and the flavor anomaly in $\overline{B} \to D^{(*)} l \overline{\nu}$ through the popular $SU(2)_L$-singlet vector LQ coupled primarily to third-generation fermions. In the LQ interactions, there is one CP-violating phase which is required to accommodate the $R_{D^{(*)}}$ anomaly, and hence CP-violating phenomena are inevitably predicted. We investigated various EDMs and found that neutron and proton EDMs are induced with opposite signs, and predicted magnitudes are within reach of the sensitivities of future experiments.

Correlations with other CPV phenomena, *e.g.*, $\Delta A_{CP}(B \to X_s\gamma)$, will also be interesting and we leave them as a future work. It is known that the remaining discrepancies in $b \to s\ell^+\ell^-$ could also be solved by the U_1 LQ at one-loop level [100]. Going beyond the leading-log approximation is necessary for the presence of vector-like fermions, and it will also be a part of future work.

ACKNOWLEDGEMENTS

We thank Yohei Ema, Ulrich Nierste, Shohei Okawa, and Maxim Pospelov for their valuable comments and discussions. We also appreciate Felix Wilsch for the technical support of `HighPT`. S. I. enjoys the support from the Deutsche Forschungsgemeinschaft (DFG, German Research Foundation) under grant 396021762-TRR 257. S. I. would like to appreciate the "hot" hospitality at Universidad de Barcelona where the last stage of this project was made. T. K. was supported by the Grant-in-Aid for Scientific Research (C) from the Ministry of Education, Culture, Sports, Science, and Technology (MEXT), Japan, No. 21K03572. This work is also supported by the Japan Society for the Promotion of Science (JSPS) Core-to-Core Program, No. JPJSCCA20200002.

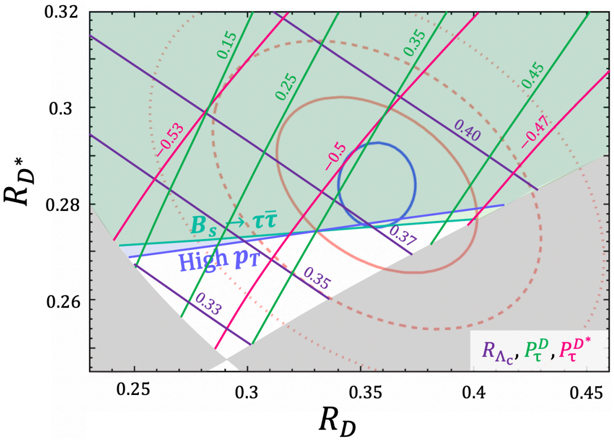

FIG. 5. Correlations with the τ polarization asymmetries, P_τ^D and $P_\tau^{D^*}$, and the LFU violation in $\Lambda_b \to \Lambda_c l\overline{\nu}$, R_{Λ_c}, are shown on the plane of R_D–R_{D^*} by the green, magenta, and purple contours, respectively.

Appendix A: Other $b \to c\tau\overline{\nu}$ observables

In this appendix, other related observables in $b \to c\tau\overline{\nu}$ are discussed in the simplified U_1 LQ model. In Fig. 5, the τ polarization asymmetries in $\overline{B} \to D^{(*)}\tau\overline{\nu}$, P_τ^D and $P_\tau^{D^*}$ [102, 103], and the LFU violation in $\Lambda_b \to \Lambda_c l\overline{\nu}$, $R_{\Lambda_c} \equiv \mathcal{B}(\Lambda_b \to \Lambda_c\tau\overline{\nu}_\tau)/\mathcal{B}(\Lambda_b \to \Lambda_c\ell\overline{\nu}_\ell)$, are shown by the green, magenta, and purple contours, respectively.

It is found that $P_\tau^{D^*}$ cannot deviate from the SM prediction $P_{\tau,\mathrm{SM}}^{D^*} \simeq -0.50$, while P_τ^D can deviate from $P_{\tau,\mathrm{SM}}^D \simeq 0.33$ which will be probed by the Belle II with good accuracy [104]. On the other hand, a large value of R_{Λ_c} is expected compared to the SM prediction, $R_{\Lambda_c}^{\mathrm{SM}} \simeq 0.32$ [105]. This behavior is consistent with a sum rule prediction [106–108], and it should also be a smoking-gun signal in the LHCb [109]. Note that the D^* longitudinal polarization ratio in $\overline{B} \to D^*\tau\overline{\nu}$, $F_L^{D^*}$ [102, 110], is also predicted. It is, however, found that the U_1 LQ effect is tiny, $\Delta F_L^{D^*} = 0.01$ [41, 111], and it is smaller than the Belle II sensitivity [26].

---

[1] **BaBar** Collaboration, *Evidence for an excess of $\bar{B} \to D^{(*)}\tau^-\bar{\nu}_\tau$ decays*, Phys. Rev. Lett. **109** (2012) 101802 [`arXiv:1205.5442`].

[2] **BaBar** Collaboration, *Measurement of an Excess of $\bar{B} \to D^{(*)}\tau^-\bar{\nu}_\tau$ Decays and Implications for Charged Higgs Bosons*, Phys. Rev. D **88** (2013) 072012 [`arXiv:1303.0571`].

[3] **Belle** Collaboration, *Measurement of the branching ratio of $\bar{B} \to D^{(*)}\tau^-\bar{\nu}_\tau$ relative to $\bar{B} \to D^{(*)}\ell^-\bar{\nu}_\ell$ decays with hadronic tagging at Belle*, Phys. Rev. D **92** (2015) 072014 [`arXiv:1507.03233`].

[4] **Belle** Collaboration, *Measurement of the τ lepton polarization and $R(D^*)$ in the decay $\bar{B} \to D^*\tau^-\bar{\nu}_\tau$*, Phys. Rev. Lett. **118** (2017) 211801 [`arXiv:1612.00529`].

[5] **Belle** Collaboration, *Measurement of the τ lepton polarization and $R(D^*)$ in the decay $\bar{B} \to D^*\tau^-\bar{\nu}_\tau$ with one-prong hadronic τ decays at Belle*, Phys. Rev. D **97** (2018) 012004 [`arXiv:1709.00129`].

[6] **Belle** Collaboration, *Measurement of $\mathcal{R}(D)$ and $\mathcal{R}(D^*)$ with a semileptonic tagging method.* `arXiv:1904.08794`.

[7] **Belle** Collaboration, *Measurement of $\mathcal{R}(D)$ and $\mathcal{R}(D^*)$ with a semileptonic tagging method*, Phys. Rev. Lett. **124** (2020) 161803 [`arXiv:1910.05864`].

[8] **LHCb** Collaboration, *Measurement of the ratio of branching fractions $\mathcal{B}(\bar{B}^0 \to D^{*+}\tau^-\bar{\nu}_\tau)/\mathcal{B}(\bar{B}^0 \to D^{*+}\mu^-\bar{\nu}_\mu)$*, Phys. Rev. Lett. **115** (2015) 111803 [`arXiv:1506.08614`]. [Erratum: Phys.Rev.Lett. 115, 159901 (2015)].

[9] **LHCb** Collaboration, *Measurement of the ratio of the $B^0 \to D^{*-}\tau^+\nu_\tau$ and $B^0 \to D^{*-}\mu^+\nu_\mu$ branching fractions using three-prong τ-lepton decays*, Phys. Rev. Lett. **120** (2018) 171802 [`arXiv:1708.08856`].

[10] **LHCb** Collaboration, *Test of Lepton Flavor Universality by the measurement of the $B^0 \to D^{*-}\tau^+\nu_\tau$ branching fraction using three-prong τ decays*, Phys. Rev. D **97** (2018) 072013 [`arXiv:1711.02505`].

[11] **LHCb** Collaboration, *Measurement of the ratios of branching fractions $\mathcal{R}(D^*)$ and $\mathcal{R}(D^0)$.* `arXiv:2302.02886`.

[12] **LHCb** Collaboration, *Test of lepton flavour universality using $B^0 \to D^{*-}\tau^+\nu_\tau$ decays with hadronic τ channels.* `arXiv:2305.01463`.

[13] **Belle II** Collaboration, *Recent Belle II results on semileptonic B decays and tests of lepton-flavor universality.* `https://indico.cern.ch/event/1114856/contributions/5423684/`.

[14] **Heavy Flavor Averaging Group, HFLAV** Collaboration, *Averages of b-hadron, c-hadron, and τ-lepton properties as of 2021*, Phys. Rev. D **107** (2023) 052008 [`arXiv:2206.07501`].

[15] **HFLAV** Collaboration. “Preliminary average of $R(D)$ and $R(D^*)$ for Summer 2023” at `https://hflav-eos.web.cern.ch/hflav-eos/semi/summer23/html/RDsDsstar/RDRDs.html`.

[16] M. Bordone, N. Gubernari, D. van Dyk, and M. Jung, *Heavy-Quark expansion for $\bar{B}_s \to D_s^{(*)}$ form factors and unitarity bounds beyond the $SU(3)_F$ limit*, Eur. Phys. J. C **80** (2020) 347 [`arXiv:1912.09335`].

[17] S. Iguro and R. Watanabe, *Bayesian fit analysis to full distribution data of $\bar{B} \to D^{(*)}\ell\bar{\nu}$: $|V_{cb}|$ determination and New Physics constraints*, JHEP **08** (2020) 006 [`arXiv:2004.10208`].

[18] F. U. Bernlochner, *et al.*, *Constrained second-order power corrections in HQET: R(D(*)), —Vcb—, and new physics*, Phys. Rev. D **106** (2022) 096015 [`arXiv:2206.11281`].

[19] S. Iguro, T. Kitahara, and R. Watanabe, *Global fit to $b \to c\tau\nu$ anomalies 2022 mid-autumn.* `arXiv:2210.10751`.

[20] D. London and J. Matias, *B Flavour Anomalies: 2021 Theoretical Status Report,* Ann. Rev. Nucl. Part. Sci. **72** (2022) 37–68 [`arXiv:2110.13270`].

[21] L. Di Luzio, A. Greljo, and M. Nardecchia, *Gauge leptoquark as the origin of B-physics anomalies,* Phys. Rev. D **96** (2017) 115011 [`arXiv:1708.08450`].

[22] M. Bordone, C. Cornella, J. Fuentes-Martin, and G. Isidori, *A three-site gauge model for flavor hierarchies and flavor anomalies,* Phys. Lett. B **779** (2018) 317–323 [`arXiv:1712.01368`].

[23] M. Bordone, C. Cornella, J. Fuentes-Martín, and G. Isidori, *Low-energy signatures of the* PS^3 *model: from B-physics anomalies to LFV,* JHEP **10** (2018) 148 [`arXiv:1805.09328`].

[24] L. Calibbi, A. Crivellin, and T. Li, *Model of vector leptoquarks in view of the B-physics anomalies,* Phys. Rev. D **98** (2018) 115002 [`arXiv:1709.00692`].

[25] B. Capdevila, A. Crivellin, S. Descotes-Genon, L. Hofer, and J. Matias, *Searching for New Physics with* $b \to s\tau^+\tau^-$ *processes,* Phys. Rev. Lett. **120** (2018) 181802 [`arXiv:1712.01919`].

[26] **Belle-II** Collaboration, *The Belle II Physics Book,* PTEP **2019** (2019) 123C01 [`arXiv:1808.10567`]. [Erratum: PTEP 2020, 029201 (2020)].

[27] A. Cerri *et al.*, *Report from Working Group 4: Opportunities in Flavour Physics at the HL-LHC and HE-LHC,* CERN Yellow Rep. Monogr. **7** (2019) 867–1158 [`arXiv:1812.07638`].

[28] P. Q. Hung, A. J. Buras, and J. D. Bjorken, *Petite Unification of Quarks and Leptons,* Phys. Rev. D **25** (1982) 805.

[29] G. Valencia and S. Willenbrock, *Quark - lepton unification and rare meson decays,* Phys. Rev. D **50** (1994) 6843–6848 [`hep-ph/9409201`].

[30] A. Pomarol and D. Tommasini, *Horizontal symmetries for the supersymmetric flavor problem,* Nucl. Phys. B **466** (1996) 3–24 [`hep-ph/9507462`].

[31] R. Barbieri, G. R. Dvali, and L. J. Hall, *Predictions from a U(2) flavor symmetry in supersymmetric theories,* Phys. Lett. B **377** (1996) 76–82 [`hep-ph/9512388`].

[32] R. Barbieri, G. Isidori, J. Jones-Perez, P. Lodone, and D. M. Straub, $U(2)$ *and Minimal Flavour Violation in Supersymmetry,* Eur. Phys. J. C **71** (2011) 1725 [`arXiv:1105.2296`].

[33] R. Barbieri, G. Isidori, A. Pattori, and F. Senia, *Anomalies in B-decays and* $U(2)$ *flavour symmetry,* Eur. Phys. J. C **76** (2016) 67 [`arXiv:1512.01560`].

[34] G. Panico, A. Pomarol, and M. Riembau, *EFT approach to the electron Electric Dipole Moment at the two-loop level,* JHEP **04** (2019) 090 [`arXiv:1810.09413`].

[35] W. Altmannshofer, S. Gori, H. H. Patel, S. Profumo, and D. Tuckler, *Electric dipole moments in a leptoquark scenario for the B-physics anomalies,* JHEP **05** (2020) 069 [`arXiv:2002.01400`].

[36] K. Fuyuto, M. Ramsey-Musolf, and T. Shen, *Electric Dipole Moments from CP-Violating Scalar Leptoquark Interactions,* Phys. Lett. B **788** (2019) 52–57 [`arXiv:1804.01137`].

[37] W. Dekens, J. de Vries, M. Jung, and K. K. Vos, *The phenomenology of electric dipole moments in models of scalar leptoquarks,* JHEP **01** (2019) 069 [`arXiv:1809.09114`].

[38] A. Crivellin and F. Saturnino, *Correlating tauonic B decays with the neutron electric dipole moment via a scalar leptoquark,* Phys. Rev. D **100** (2019) 115014 [`arXiv:1905.08257`].

[39] K. S. Babu, P. S. B. Dev, S. Jana, and A. Thapa, *Unified framework for B-anomalies, muon* $g-2$ *and neutrino masses,* JHEP **03** (2021) 179 [`arXiv:2009.01771`].

[40] C. Cornella, J. Fuentes-Martin, and G. Isidori, *Revisiting the vector leptoquark explanation of the B-physics anomalies,* JHEP **07** (2019) 168 [`arXiv:1903.11517`].

[41] S. Iguro, T. Kitahara, Y. Omura, R. Watanabe, and K. Yamamoto, D^* *polarization vs.* $R_{D^{(*)}}$ *anomalies in the leptoquark models,* JHEP **02** (2019) 194 [`arXiv:1811.08899`].

[42] F. S. Queiroz and W. Shepherd, *New Physics Contributions to the Muon Anomalous Magnetic Moment: A Numerical Code,* Phys. Rev. D **89** (2014) 095024 [`arXiv:1403.2309`].

[43] K. Kowalska, E. M. Sessolo, and Y. Yamamoto, *Constraints on charmphilic solutions to the muon g-2 with leptoquarks,* Phys. Rev. D **99** (2019) 055007 [`arXiv:1812.06851`].

[44] U. Haisch and G. Koole, *Beautiful and charming chromodipole moments,* JHEP **09** (2021) 133 [`arXiv:2106.01289`].

[45] W. Dekens and J. de Vries, *Renormalization Group Running of Dimension-Six Sources of Parity and Time-Reversal Violation,* JHEP **05** (2013) 149 [`arXiv:1303.3156`].

[46] A. G. Grozin, I. B. Khriplovich, and A. S. Rudenko, *Electric dipole moments, from e to tau,* Phys. Atom. Nucl. **72** (2009) 1203–1205 [`arXiv:0811.1641`].

[47] Y. Ema, T. Gao, and M. Pospelov, *Improved Indirect Limits on Muon Electric Dipole Moment,* Phys. Rev. Lett. **128** (2022) 131803 [`arXiv:2108.05398`].

[48] Y. Ema, T. Gao, and M. Pospelov, *Improved indirect limits on charm and bottom quark EDMs,* JHEP **07** (2022) 106 [`arXiv:2205.11532`].

[49] M. Pospelov and A. Ritz, *CKM benchmarks for electron electric dipole moment experiments,* Phys. Rev. D **89** (2014) 056006 [`arXiv:1311.5537`].

[50] K. Kaneta, N. Nagata, K. A. Olive, M. Pospelov, and L. Velasco-Sevilla, *Quantifying limits on CP violating phases from EDMs in supersymmetry,* JHEP **03** (2023) 250 [`arXiv:2303.02822`].

[51] Y. Ema, T. Gao, and M. Pospelov, *Reevaluation of heavy-fermion-induced electron EDM at three loops,* Phys. Lett. B **835** (2022) 137496 [`arXiv:2207.01679`].

[52] T. S. Roussy *et al.*, *A new bound on the electron's electric dipole moment,* Science **381** (2023) 46 [`arXiv:2212.11841`].

[53] G. Boyd, A. K. Gupta, S. P. Trivedi, and M. B. Wise, *Effective Hamiltonian for the Electric Dipole Moment of the Neutron,* Phys. Lett. B **241** (1990) 584–588.

[54] E. Braaten, C.-S. Li, and T.-C. Yuan, *The Evolution of Weinberg's Gluonic CP Violation Operator,* Phys. Rev. Lett. **64** (1990) 1709.

[55] D. Chang, W.-Y. Keung, C. S. Li, and T. C. Yuan, *QCD Corrections to CP Violation From Color Electric Dipole Moment of b Quark,* Phys. Lett. B **241** (1990) 589–592.

[56] M. Pospelov and A. Ritz, *Neutron EDM from electric*

and chromoelectric dipole moments of quarks, Phys. Rev. D **63** (2001) 073015 [`hep-ph/0010037`].

[57] M. Pospelov and A. Ritz, *Electric dipole moments as probes of new physics,* Annals Phys. **318** (2005) 119–169 [`hep-ph/0504231`].

[58] J. Hisano, J. Y. Lee, N. Nagata, and Y. Shimizu, *Reevaluation of Neutron Electric Dipole Moment with QCD Sum Rules,* Phys. Rev. D **85** (2012) 114044 [`arXiv:1204.2653`].

[59] K. Fuyuto, J. Hisano, N. Nagata, and K. Tsumura, *QCD Corrections to Quark (Chromo)Electric Dipole Moments in High-scale Supersymmetry,* JHEP **12** (2013) 010 [`arXiv:1308.6493`].

[60] C. Alexandrou, *et al.*, *Nucleon axial, tensor, and scalar charges and σ-terms in lattice QCD,* Phys. Rev. D **102** (2020) 054517 [`arXiv:1909.00485`].

[61] D. A. Demir, M. Pospelov, and A. Ritz, *Hadronic EDMs, the Weinberg operator, and light gluinos,* Phys. Rev. D **67** (2003) 015007 [`hep-ph/0208257`].

[62] U. Haisch and A. Hala, *Sum rules for CP-violating operators of Weinberg type,* JHEP **11** (2019) 154 [`arXiv:1909.08955`].

[63] N. Yamanaka and E. Hiyama, *Weinberg operator contribution to the nucleon electric dipole moment in the quark model,* Phys. Rev. D **103** (2021) 035023 [`arXiv:2011.02531`].

[64] T. Bhattacharya, V. Cirigliano, R. Gupta, and B. Yoon, *Quark Chromoelectric Dipole Moment Contribution to the Neutron Electric Dipole Moment,* PoS **LATTICE2016** (2016) 225 [`arXiv:1612.08438`].

[65] B. Yoon, T. Bhattacharya, and R. Gupta, *Neutron Electric Dipole Moment on the Lattice,* EPJ Web Conf. **175** (2018) 01014 [`arXiv:1712.08557`].

[66] E. Mereghetti, *Lattice QCD and nuclear physics for searches of physics beyond the Standard Model,* PoS **LATTICE2018** (2019) 002 [`arXiv:1812.11238`].

[67] B. Yoon, T. Bhattacharya, V. Cirigliano, and R. Gupta, *Neutron Electric Dipole Moments with Clover Fermions,* PoS **LATTICE2019** (2020) 243 [`arXiv:2003.05390`].

[68] A. Todaro, C. Alexandrou, A. Athenodorou, and K. Hadjiannakou, *A lattice QCD determination of the neutron electric dipole moment at the physical point,* PoS **LATTICE2021** (2022) 120 [`arXiv:2112.03989`].

[69] T. Bhattacharya, V. Cirigliano, R. Gupta, E. Mereghetti, and B. Yoon, *Calculation of neutron electric dipole moment due to the QCD topological term, Weinberg three-gluon operator and the quark chromoelectric moment,* PoS **LATTICE2021** (2022) 567 [`arXiv:2203.03746`].

[70] T. Bhattacharya, V. Cirigliano, R. Gupta, E. Mereghetti, and B. Yoon, *nEDM from the theta-term and chromoEDM operators,* PoS **LATTICE2022** (2023) 304 [`arXiv:2301.08161`].

[71] R. Alarcon *et al.* in *Snowmass 2021.* 2022. `arXiv:2203.08103`.

[72] C. Abel *et al.*, *Measurement of the Permanent Electric Dipole Moment of the Neutron,* Phys. Rev. Lett. **124** (2020) 081803 [`arXiv:2001.11966`].

[73] **n2EDM** Collaboration, *The design of the n2EDM experiment: nEDM Collaboration,* Eur. Phys. J. C **81** (2021) 512 [`arXiv:2101.08730`].

[74] J. W. Martin, *Current status of neutron electric dipole moment experiments,* J. Phys. Conf. Ser. **1643** (2020) 012002.

[75] T. M. Ito *et al.*, *Performance of the upgraded ultracold neutron source at Los Alamos National Laboratory and its implication for a possible neutron electric dipole moment experiment,* Phys. Rev. C **97** (2018) 012501 [`arXiv:1710.05182`].

[76] D. Wurm *et al.*, *The PanEDM Neutron Electric Dipole Moment Experiment at the ILL,* EPJ Web Conf. **219** (2019) 02006 [`arXiv:1911.09161`].

[77] **nEDM** Collaboration, *A New Cryogenic Apparatus to Search for the Neutron Electric Dipole Moment,* JINST **14** (2019) P11017 [`arXiv:1908.09937`].

[78] B. K. Sahoo, *Improved limits on the hadronic and semihadronic CP violating parameters and role of a dark force carrier in the electric dipole moment of ^{199}Hg,* Phys. Rev. D **95** (2017) 013002 [`arXiv:1612.09371`].

[79] **CPEDM** Collaboration, *Storage ring to search for electricdipole moments of charged particles: Feasibility study*. CERN, Geneva, 2021. `arXiv:1912.07881`.

[80] J. Alexander *et al.*, *The storage ring proton EDM experiment.* `arXiv:2205.00830`.

[81] J. Aebischer, M. Fael, C. Greub, and J. Virto, *B physics Beyond the Standard Model at One Loop: Complete Renormalization Group Evolution below the Electroweak Scale,* JHEP **09** (2017) 158 [`arXiv:1704.06639`].

[82] M. González-Alonso, J. Martin Camalich, and K. Mimouni, *Renormalization-group evolution of new physics contributions to (semi)leptonic meson decays,* Phys. Lett. B **772** (2017) 777–785 [`arXiv:1706.00410`].

[83] J. Aebischer, A. Crivellin, and C. Greub, *QCD improved matching for semileptonic B decays with leptoquarks,* Phys. Rev. D **99** (2019) 055002 [`arXiv:1811.08907`].

[84] **LHCb** Collaboration, *Search for the decays $B_s^0 \to \tau^+\tau^-$ and $B^0 \to \tau^+\tau^-$,* Phys. Rev. Lett. **118** (2017) 251802 [`arXiv:1703.02508`].

[85] **LHCb** Collaboration, *Physics case for an LHCb Upgrade II - Opportunities in flavour physics, and beyond, in the HL-LHC era.* `arXiv:1808.08865`.

[86] L. Allwicher, D. A. Faroughy, F. Jaffredo, O. Sumensari, and F. Wilsch, *HighPT: A tool for high-pT Drell-Yan tails beyond the standard model,* Comput. Phys. Commun. **289** (2023) 108749 [`arXiv:2207.10756`].

[87] **ATLAS** Collaboration, *Search for heavy Higgs bosons decaying into two tau leptons with the ATLAS detector using pp collisions at $\sqrt{s} = 13$ TeV,* Phys. Rev. Lett. **125** (2020) 051801 [`arXiv:2002.12223`].

[88] M. J. Baker, J. Fuentes-Martín, G. Isidori, and M. König, *High- p_T signatures in vector–leptoquark models,* Eur. Phys. J. C **79** (2019) 334 [`arXiv:1901.10480`].

[89] A. Bhaskar, D. Das, T. Mandal, S. Mitra, and C. Neeraj, *Precise limits on the charge-2/3 U1 vector leptoquark,* Phys. Rev. D **104** (2021) 035016 [`arXiv:2101.12069`].

[90] **CMS** Collaboration, *The search for a third-generation leptoquark coupling to a τ lepton and a b quark through single, pair and nonresonant production at* $\sqrt{s} = 13$ TeV. `https://cds.cern.ch/record/2815309`.

[91] **CMS** Collaboration, *Searches for additional Higgs*

bosons and for vector leptoquarks in $\tau\tau$ final states in proton-proton collisions at $\sqrt{s} = 13$ TeV. arXiv:2208.02717.

[92] **CMS** Collaboration, *A flavor for leptoquarks.* https://indico.cern.ch/event/1114856/contributions/5360087/.

[93] A. Greljo, J. Martin Camalich, and J. D. Ruiz-Álvarez, *Mono-τ Signatures at the LHC Constrain Explanations of B-decay Anomalies,* Phys. Rev. Lett. **122** (2019) 131803 [arXiv:1811.07920].

[94] S. Iguro, M. Takeuchi, and R. Watanabe, *Testing leptoquark/EFT in $\bar{B} \to D^{(*)} l\bar{\nu}$ at the LHC,* Eur. Phys. J. C **81** (2021) 406 [arXiv:2011.02486].

[95] D. Marzocca, U. Min, and M. Son, *Bottom-Flavored Mono-Tau Tails at the LHC,* JHEP **12** (2020) 035 [arXiv:2008.07541].

[96] M. Endo, S. Iguro, T. Kitahara, M. Takeuchi, and R. Watanabe, *Non-resonant new physics search at the LHC for the $b \to c\tau\nu$ anomalies,* JHEP **02** (2022) 106 [arXiv:2111.04748].

[97] L. Di Luzio, J. Fuentes-Martin, A. Greljo, M. Nardecchia, and S. Renner, *Maximal Flavour Violation: a Cabibbo mechanism for leptoquarks,* JHEP **11** (2018) 081 [arXiv:1808.00942].

[98] J. Fuentes-Martín, G. Isidori, M. König, and N. Selimović, *Vector Leptoquarks Beyond Tree Level III: Vector-like Fermions and Flavor-Changing Transitions,* Phys. Rev. D **102** (2020) 115015 [arXiv:2009.11296].

[99] D. Marzocca, *Addressing the B-physics anomalies in a fundamental Composite Higgs Model,* JHEP **07** (2018) 121 [arXiv:1803.10972].

[100] A. Crivellin, C. Greub, D. Müller, and F. Saturnino, *Importance of Loop Effects in Explaining the Accumulated Evidence for New Physics in B Decays with a Vector Leptoquark,* Phys. Rev. Lett. **122** (2019) 011805 [arXiv:1807.02068].

[101] S. Iguro, J. Kawamura, S. Okawa, and Y. Omura, *Importance of vector leptoquark-scalar box diagrams in Pati-Salam unification with vector-like families,* JHEP **07** (2022) 022 [arXiv:2201.04638].

[102] M. Tanaka and R. Watanabe, *New physics in the weak interaction of $\bar{B} \to D^{(*)}\tau\bar{\nu}$,* Phys. Rev. D **87** (2013) 034028 [arXiv:1212.1878].

[103] P. Asadi, M. R. Buckley, and D. Shih, *Asymmetry Observables and the Origin of $R_{D^{(*)}}$ Anomalies,* Phys. Rev. D **99** (2019) 035015 [arXiv:1810.06597].

[104] R. Alonso, J. Martin Camalich, and S. Westhoff, *Tau properties in $B \to D\tau\nu$ from visible final-state kinematics,* Phys. Rev. D **95** (2017) 093006 [arXiv:1702.02773].

[105] F. U. Bernlochner, Z. Ligeti, D. J. Robinson, and W. L. Sutcliffe, *New predictions for $\Lambda_b \to \Lambda_c$ semileptonic decays and tests of heavy quark symmetry,* Phys. Rev. Lett. **121** (2018) 202001 [arXiv:1808.09464].

[106] M. Blanke, *et al.*, *Impact of polarization observables and $B_c \to \tau\nu$ on new physics explanations of the $b \to c\tau\nu$ anomaly,* Phys. Rev. D **99** (2019) 075006 [arXiv:1811.09603].

[107] M. Blanke, *et al.*, *Addendum to "Impact of polarization observables and $B_c \to \tau\nu$ on new physics explanations of the $b \to c\tau\nu$ anomaly",* Phys. Rev. D **100** (2019) 035035 [arXiv:1905.08253].

[108] M. Fedele, *et al.*, *Impact of $\Lambda b{\to}\Lambda c\tau\nu$ measurement on new physics in $b{\to}cl\nu$ transitions,* Phys. Rev. D **107** (2023) 055005 [arXiv:2211.14172].

[109] **LHCb** Collaboration, *Observation of the decay $\Lambda_b^0 \to \Lambda_c^+\tau^-\overline{\nu}_\tau$,* Phys. Rev. Lett. **128** (2022) 191803 [arXiv:2201.03497].

[110] **Belle** Collaboration in *10th International Workshop on the CKM Unitarity Triangle.* 2019. arXiv:1903.03102.

[111] J. Fuentes-Martín, G. Isidori, J. Pagès, and K. Yamamoto, *With or without U(2)? Probing non-standard flavor and helicity structures in semileptonic B decays,* Phys. Lett. B **800** (2020) 135080 [arXiv:1909.02519].